Int. J. Multiphase Flow Vol. 16, No. 3, pp. 495–513, 1990
Printed in Great Britain.

0301-9322/90 $3.00 + 0.00

TEMPERATURE DISTRIBUTION AND HEAT TRANSFER IN A PARTICLE–FLUID FLOW PAST A HEATED HORIZONTAL PLATE

N. APAZIDIS
Department of Mechanics, Royal Institute of Technology, 100 44 Stockholm, Sweden

(*Received* 9 *February* 1989; *in revised form* 25 *November* 1989)

Abstract—The temperature distribution in a laminar two-phase flow of a particle–fluid mixture over a heated horizontal plate is considered. Analytical expressions for the temperature fields and heat fluxes in each phase are obtained. It is found that the temperature distribution in a two-phase mixture flow differs from the corresponding single-phase case. Temperature profiles of the phases are independent of the distance along the plate and controlled by such mixture parameters as the particle size and concentration, the density ratio between the phases and the value of the Prandtl number. Moreover, the temperature fields of the phases in the mixture flow are independent of the horizontal velocity components and have a structure similar to that of a velocity profile of a single-phase flow over a flat plate at zero incidence with uniform suction.

Key Words: two-phase flow, particle–fluid mixture, heated horizontal plate, thermal boundary layer, temperature, heat flux

1. INTRODUCTION

The velocity distribution in a laminar two-phase mixture flow over an infinite plate has been considered previously by Apazidis (1985). The investigation was based on a continuum description of each phase, the solid particles and the carrier fluid, by means of separate equations of mass and momentum balance, the latter coupled through an interaction force between the phases. Such a continuum model is supplied by the works of, for example, Ishii (1975), Drew (1979, 1983) and Drumheller & Bedford (1980).

This type of laminar two-phase mixture flow develops a boundary layer with a structure that is different from its single-phase counterpart. The continuity and momentum equations give a velocity distribution which is independent of the distance along the plate and has a simple structure, similar to that of a single-phase flow over a flat plate at zero incidence with uniform suction along the plate (e.g. Schlichting 1968). In both cases the constant streaming motion in the direction transverse to the plate allows the existence of a simple particular solution of the system of continuity and momentum equations for which the velocity is independent of the current length. In the present case, however, this velocity boundary layer exists at the interface between the dense sediment collected on the plate and the mixture above it. The interface and thus the boundary layer are propagating in the upward direction with a velocity of growth of the sediment layer, defined by a particle size and concentration and the density ratio between the phases. The thickness of this boundary layer may be measured in particle radii and depends on the particle concentration, the value of the particle Reynolds number and the density ratio between the phases.

In the present work we will analyse the structure of the temperature distribution and heat transfer in a similar laminar two-phase streaming motion over a flat infinite horizontal plate. We will add energy equations for each phase to the mass and momentum conservation equations. General forms of the energy equations may be found in the works of, for example, Ishii (1975), Bennon & Incropera (1987), Drumheller & Bedford (1980), Soo (1965) and Sha & Soo (1978).

It is found that the form of the equations describing the temperature distribution in a two-phase mixture flow is, as in the single-phase case, the same as those of the velocity boundary layer, provided that the friction heat is neglected. The structure of the temperature distribution in a two-phase mixture flow differs in two important respects from its single-phase counterpart: (1) temperature profiles are independent of the distance along the plate; and (2) the temperature distribution in each phase is independent of the horizontal velocity components. The depth of

penetration of the temperature profiles in the two-phase case is controlled by the volume fraction of particles, the value of the particle Reynolds number, the density ratio of the phases and the value of the Prandtl number.

2. GOVERNING EQUATIONS

Consider a laminar flow of a mixture of solid spherical particles homogeneously distributed in a continuous carrier fluid or gas past a heated horizontal plate with a constant temperature T_w. The mixture is assumed to be in thermal equilibrium with the constituents having the common temperature T_∞ sufficiently far from the plate. The density difference between the phases in the presence of a gravity field perpendicular to the plate introduces separational motion of the phases in the vertical direction. This separational motion consists of a flow of heavy particles in the downward direction, forming a layer of dense sediment on the plate, and a flow of fluid in the opposite upward direction. This separational motion due to the density difference between the phases has been considered previously by Apazidis (1985). We will adopt this analysis here and make use of the calculated velocity distributions in the particle and fluid phases. The goal of the present work is to incorporate the energy equations for each constituent of the mixture in the model. Solutions of the latter together with the mass and momentum balance equations will give the temperature distributions in each phase as well as the separate and total heat fluxes in the mixture.

The present analysis is based on the following assumptions:

(1) The phases are viewed as two interacting continua obeying separate equations of balance of mass, momentum and energy.
(2) The carrier phase is a viscous incompressible fluid.
(3) The particles are solid spheres of equal radii.
(4) The particle concentration is constant in time and space and "dilute" in the sense that the inter-particle collisions are insignificant and the particle flow is controlled by the momentum and energy exchange with the continuous carrier phase.
(5) The flow of both phases is laminar, with particle Reynolds number <1.
(6) The particle size is large enough to neglect the Brownian motion.

On the basis of these assumptions we formulate the balance equations governing the two-dimensional flow of a mixture past a heated horizontal plate. The flow is assumed to be homogeneous in the horizontal direction with the flow variables being functions of the vertical coordinate y and time t alone:

Balance of mass,
particles

$$\alpha_t + (\alpha v_d)_y = 0; \tag{1}$$

and

fluid

$$-\alpha_t + [(1-\alpha)v_c]_y = 0. \tag{2}$$

Balance of momentum,
particles

$$\alpha\rho_d(u_{dt} + v_d u_{dy}) = \tfrac{9}{2} f(\alpha)\frac{\mu_c}{a^2}(u_c - u_d) \tag{3}$$

and

$$\alpha\rho_d(v_{dt} + v_d v_{dy}) = -\alpha\rho_d g - \alpha p_y + \tfrac{9}{2} f(\alpha)\frac{\mu_c}{a^2}(v_c - v_d); \tag{4}$$

and

fluid

$$(1-\alpha)\rho_c(u_{ct}+v_c u_{cy}) = (1-\alpha)\mu_c u_{cyy} - \tfrac{9}{2}f(\alpha)\frac{\mu_c}{a^2}(u_c-u_d) \quad [5]$$

and

$$(1-\alpha)\rho_c(v_{ct}+v_c v_{cy}) = -(1-\alpha)\rho_c g - (1-\alpha)p_y + (1-\alpha)\mu_c v_{cyy} - \tfrac{9}{2}f(\alpha)\frac{\mu_c}{a^2}(v_c-v_d). \quad [6]$$

Due to the assumption, (4), of a "dilute" particle phase consisting of solid spherical particles of equal size, homogeneously distributed in a continuous carrier phase, the stress tensor for the dispersed phase is taken to be zero (e.g. Ishii 1975; Drew 1983). The interaction force between the phases in the present model is the classical Stokes' drag on a single spherical particle modified by a correction factor $f(\alpha)$, accounting for the finite volume fraction of the dispersed phase. Contributions to the interaction force between the phases, such as the shear-lift force (Saffman 1965), the virtual mass force (Zuber 1964) and the spin-lift force (Rubinow & Keller 1961), are negligible compared to the Stoke's drag under the present assumption of small particle Reynolds number (Apazidis 1985, 1988). Tam (1969) obtained an expression for $f(\alpha)$ in the case of spherical particles,

$$f(\alpha) = \frac{4+3(8\alpha-3\alpha^2)^{1/2}+3\alpha}{(2-3\alpha)^2}\alpha. \quad [7]$$

Balance of energy,

particles

$$\alpha\rho_d c_d(T_{dt}+v_d T_{dy}) = \xi\frac{9}{2}\frac{\mu_c}{a^2}f(\alpha)[(u_c-u_d)^2+(v_c-v_d)^2] + 3\frac{\lambda_c}{a^2}\alpha(T_c-T_d); \quad [8]$$

fluid

$$(1-\alpha)\rho_c c_c(T_{ct}+v_c T_{cy}) = (1-\alpha)\mu_c(u_{cy})^2 + (1-\alpha)T_{cyy} + (1-\xi)\frac{9}{2}\frac{\mu_c}{a^2}f(\alpha)[(u_c-u_d)^2+(v_c-v_d)^2] - 3\frac{\lambda_c}{a^2}\alpha(T_c-T_d). \quad [9]$$

Similarly to Ishii *et al.* (1987), we apply the general forms of the energy equations to the particle–fluid flow under the present assumptions. The first term on the r.h.s. of [8] represents the dissipation heat due to the relative motion between the phases and the second term is the heat flux between the phases. Here ξ $(0 \leqslant \xi \leqslant 1)$ is a dimensionless parameter introduced to apportion the dissipation heat between the phases (Wallis 1969). In the present work, however, we will not be forced to define the value of this parameter since the dissipation terms will subsequently be neglected.

In [1]–[9] above the following nomenclature applies: *subscripts*—d, c and t, y indicate dispersed or continuous phase and partial derivatives with respect to time and vertical coordinate, respectively; *independent variables*—t, y, a are time, vertical coordinate and particle radius, respectively; *dependent variables*—α, ρ, u, v, T, p are volume fraction of particles, density, velocity components, temperature and pressure, respectively; and *constants*—μ, λ, c and g are viscosity, thermal conductivity, specific heat and acceleration due to gravity, respectively.

Next we introduce the following set of dimensionless parameters:

$$y_* = \frac{y}{a}, \quad t_* = \frac{ga\gamma}{\nu_c}t, \quad u = \frac{ga^2\gamma}{\nu_c}U, \quad v = \frac{ga^2\gamma}{\nu_c}V, \quad \theta = \frac{T-T_\infty}{T_w-T_\infty}, \quad p = -\rho_c g y(1-\gamma P); \quad [10]$$

and

$$\gamma = \frac{\rho_d}{\rho_c}, \quad \mathrm{Re} = \frac{ga^2\gamma}{\nu_c}\frac{a}{\nu_c}, \quad \mathrm{Pr} = \frac{\nu_c}{\kappa_c}, \quad \mathrm{E} = \left(\frac{ga^2\gamma}{\nu_c}\right)^2\frac{1}{c_c(T_w-T_\infty)}, \quad k = \frac{c_d}{c_c}. \quad [11]$$

Where: $\nu_c = \mu_c/\rho_c$ and $\kappa_c = \lambda_c/(\rho_c c_c)$ are kinematic viscosity and thermal diffusivity, respectively and *dimensionless numbers*—γ, k, Re, Pr and E are density ratio, ratio of specific heats, particle Reynolds number, Prandtl number and Eckert number, respectively.

Dropping, for convenience, the asterisk notation for y and t, we write the dimensionless form of the balance equations for each phase as follows:

Balance of mass,
particles

$$\alpha_t + (\alpha V_d)_y = 0; \tag{12}$$

and

fluid

$$-\alpha_t + [(1-\alpha)V_c]_y = 0. \tag{13}$$

Balance of momentum,
particles

$$\gamma \mathrm{Re}(U_{dt} + V_d U_{dy}) = \frac{f(\alpha)}{\alpha}(U_c - U_{dy}) \tag{14}$$

and

$$\gamma \mathrm{Re}(V_{dt} + V_d V_{dy}) = -1 + P + \frac{f(\alpha)}{\alpha}(V_c - V_d); \tag{15}$$

and

fluid

$$\mathrm{Re}(U_{ct} + V_c U_{cy}) = U_{cyy} - \frac{f(\alpha)}{1-\alpha}(U_c - U_d) \tag{16}$$

and

$$\mathrm{Re}(V_{ct} + V_c V_{cy}) = P + V_{cyy} - \frac{f(\alpha)}{1-\alpha}(V_c - V_d). \tag{17}$$

Balance of energy,
particles

$$\tfrac{1}{3}\mathrm{RePr}\gamma k(\theta_{dt} + V_d\theta_{dy}) = \xi\frac{3}{2}\frac{f(\alpha)}{\alpha}\mathrm{EPr}[(U_c - U_d)^2 + (V_c - V_d)^2] + (\theta_c - \theta_d); \tag{18}$$

and

fluid

$$\tfrac{1}{3}\mathrm{RePr}(\theta_{ct} + V_c\theta_{cy}) = \tfrac{1}{3}\mathrm{EPr}(U_{cy})^2 + (1-\xi)\frac{3}{2}\frac{f(\alpha)}{1-\alpha}\mathrm{EPr}[(U_c - U_d)^2 + (V_c - V_d)^2] + \tfrac{1}{3}\theta_{cyy} - \frac{\alpha}{1-\alpha}(\theta_c - \theta_d). \tag{19}$$

We now consider for a moment the orders of magnitude of the dimensionless numbers which form the coefficients of the momentum and energy equations. Consider some examples:

(1) metal particles in gas: $\gamma \approx 10^4$, $\mathrm{Re} \approx 0.1$, $\mathrm{Pr} \approx 0.7$, $k \approx 0.45$, $\mathrm{E} \approx 10^{-6}$;
(2) metal particles in water: $\gamma \approx 10$, $\mathrm{Re} \approx 0.1$, $\mathrm{Pr} \approx 7$, $k \approx 0.1$, $\mathrm{E} \approx 10^{-10}$;
(3) metal particles in oil: $\gamma \approx 10$, $\mathrm{Re} \approx 0.1$, $\mathrm{Pr} \approx 1000$, $k \approx 0.3$, $\mathrm{E} \approx 10^{-10}$.

The ratios of the coefficients in front of the dissipation terms to the other coefficients in the energy equations are of order of magnitude $\leqslant 10^{-6}$. We therefore neglect the dissipation terms in the subsequent analysis.

By analogy with Apazidis (1985), we assume that the concentration of the dispersed phase is constant

$$\alpha = \text{const}, \tag{20}$$

which gives

$$V_{dy} = V_{cy} = 0. \tag{21}$$

We will likewise assume zero volumetric flux in the vertical direction, which is the case in the so-called batch sedimentation (e.g. Wallis 1969), i.e.

$$\alpha V_d + (1-\alpha)V_c = 0. \tag{22}$$

The momentum equations for the particles will therefore reduce to

$$\gamma \mathrm{Re}(U_{dt} + V_d U_{dy}) = \frac{f(\alpha)}{\alpha}(U_c - U_d) \tag{23}$$

and

$$\gamma \mathrm{Re} V_{dt} = -1 + P + \frac{f(\alpha)}{\alpha}(V_c - V_d); \tag{24}$$

and those for the fluid to

$$\mathrm{Re}(U_{ct} + V_c U_{cy}) = U_{cyy} - \frac{f(\alpha)}{1-\alpha}(U_c - U_d) \tag{25}$$

and

$$\mathrm{Re} V_{ct} = P + V_{cyy} - \frac{f(\alpha)}{1-\alpha}(V_c - V_d). \tag{26}$$

The energy equations for each phase take the form:

particles

$$\tfrac{1}{3}\mathrm{RePr}\gamma k(\theta_{dt} + V_d \theta_{dy}) = \theta_c - \theta_d; \tag{27}$$

and

fluid

$$\tfrac{1}{3}\mathrm{RePr}(\theta_{ct} + V_c \theta_{cy}) = \tfrac{1}{3}\theta_{cyy} - \frac{\alpha}{1-\alpha}(\theta_c - \theta_d). \tag{28}$$

The sedimentation process in a mixture moving over an infinite horizontal plate has been considered previously (Apazidis 1985). We will adopt this analysis in the present work and make use of the calculated velocity distribution of the phases in order to obtain temperature fields by means of the energy equations [27] and [28].

Here in brief are the main items of the cited analysis. The density difference between the constituents of the mixture introduces separational motion of the phases in the vertical direction, parallel to the direction of the gravity field. This motion is a combination of the particle motion in the downward direction, forming a growing layer of dense sediment on the plate, and the motion of the fluid in the opposite, upward direction. Considering the mass balance over the discontinuity surface between the dense sediment collected on the plate and the mixture above it, the velocity of propagation of the interface in the upward direction is evaluated. Since the boundary conditions for the mixture flow are formulated at the moving interface, a new coordinate system with a horizontal axis coinciding with the interface and thus propagating in the upward direction is introduced. Analytical expressions for the vertical and horizontal velocity components of the particulate and fluid phases are then obtained.

Assuming further that the vertical motion of the phases imposed by the gravity field has reached its stationary state, i.e. $V_{dt} = V_{ct} = 0$, and using [22], [24] and [26], one obtains the following expressions for the vertical velocity components:

$$V_d = -\frac{\alpha(1-\alpha)^2}{f(\alpha)} \quad [29]$$

and

$$V_c = \frac{\alpha^2(1-\alpha)}{f(\alpha)}; \quad [30]$$

and for the velocity of the interface

$$V = \frac{\alpha^2(1-\alpha)^2}{(\alpha_M - \alpha)f(\alpha)}, \quad [31]$$

where α_M is the volume fraction of particles in the dense sediment (≈ 0.6 for spheres).

The use of the new coordinate system propagating upwards with the velocity of the interface V will introduce a transformation of the independent variables t and y to the new variables t and η, where

$$\eta = y - Vt. \quad [32]$$

The energy equations [27] and [28] are then transformed to the following forms:

particles

$$A_d[\theta_{dt} - (V - V_d)\theta_{d\eta}] = \theta_c - \theta_d; \quad [33]$$

and

fluid

$$A_c[\theta_{ct} - (V - V_c)\theta_{c\eta}] = \tfrac{1}{3}\theta_{c\eta\eta} - \frac{\alpha}{1-\alpha}(\theta_c - \theta_d); \quad [34]$$

where

$$A_d = \tfrac{1}{3}\mathrm{RePr}\gamma k \quad \text{and} \quad A_c = \tfrac{1}{3}\mathrm{RePr}. \quad [35]$$

We note at this point that the energy equations under the present assumptions are independent of the velocity distribution in the horizontal direction. Since V, V_d and V_c are constants, the system [33, 34] is a system of linear partial differential equations with the boundary conditions formulated at the interface $\eta = 0$ and at infinity $\eta = \infty$.

In the following sections we will consider the temperature distribution in the phases for some simple streaming motions of the mixture over a heated horizontal plate at zero incidence.

3. STATIONARY TEMPERATURE DISTRIBUTION

We first consider a mixture flow over a horizontal plate maintained at a constant temperature T_w. We assume that both phases are at thermal equilibrium, having a common temperature T_∞ at infinity (see figure 1). The energy equations and the boundary conditions governing the stationary temperature distribution in this case are as follows:

$$-A_d(V - V_d)\theta_d' = \theta_c - \theta_d, \quad [36]$$

$$-A_c(V - V_c)\theta_c' = \tfrac{1}{3}\theta_c'' - \frac{\alpha}{1-\alpha}(\theta_c - \theta_d), \quad [37]$$

$$\eta = 0: \quad \theta_c = 1 \quad [38]$$

and

$$\eta = \infty: \quad \theta_d = \theta_c = 0, \quad [39]$$

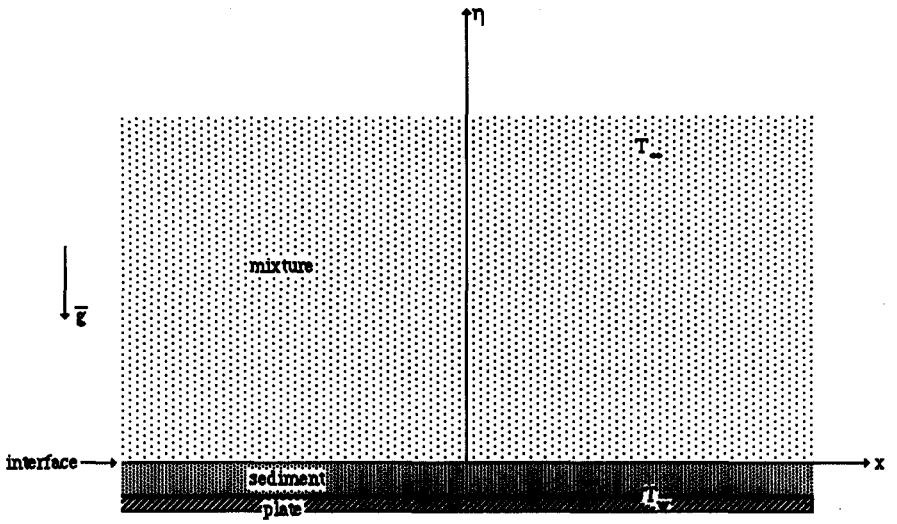

Figure 1. Problem definition.

where primes denote derivatives with respect to η. The system of energy equations is thus reduced to a system of ordinary differential equations with constant coefficients. The general solution is obtained by finding the roots of the corresponding characteristic equation, an algebraic equation of the third degree. All three roots of the equation are real:

$$r_1 = 0, \quad r_2 > 0 \quad \text{and} \quad r_3 < 0.$$

Choosing r_1 and $r_3 = r < 0$, since $\eta \geqslant 0$, and evaluating the two arbitrary constants by means of [38] and [39], we obtain a simple expression for the temperature distribution in the continuous phase

$$\theta_c = e^{r\eta}. \qquad [40]$$

The temperature distribution in the particulate phase is then evaluated by means of [28]:

$$\theta_d = \left[1 - r\frac{1-\alpha}{\alpha}A_c(V - V_c) - r^2\frac{1-\alpha}{3\alpha}\right]e^{r\eta}. \qquad [41]$$

Stationary temperature distributions in the mixture for various values of the parameters are displayed in figures 2–4 which suggest that the depth of penetration of the temperature profiles from the interface and the temperature lag of the dispersed phase from that of the continuous one are functions of the volume fraction α and the particle Reynolds number Re for a given two-phase mixture. The three considered examples are mixtures of air, water and oil with metal particles.

In the case of an air–particle mixture, as in figure 2, the particle temperature has considerable lag compared to the temperature of the air, and the depth of penetration of the temperature profiles is of order of magnitude of 100 particle radii for a dilute suspension with $\alpha = 0.001$ and $\mathrm{Re} = 1$, figure 2(a). By decreasing Re to 0.01, the thickness of the boundary layer is increased to approx. 200 particle radii, the temperature lag between the phases at the same time becomes smaller, figure 2(c). Large temperature lags between the phases are thus to be expected in thinner boundary layers. The temperature lag of the particulate phase depends on the relaxation time for energy transfer and the relative velocity between the phases. When the relaxation time and the relative velocity are large, the particles move swiftly through the fluid toward the heated plate, preserving mainly the lower temperature of the mixture layers far from the plate. This may be realized by a combination of a high density ratio, low α and a relatively large (though $\leqslant 1$) value of Re. At higher particle concentrations, the relaxation time for energy transfer becomes shorter and the relative velocity between the phases decreases, which results in smaller temperature lags between the mixture components. By decreasing Re, we obtain the similar effect of decreasing the temperature lag, this time through a decrease in the relative velocity between the phases.

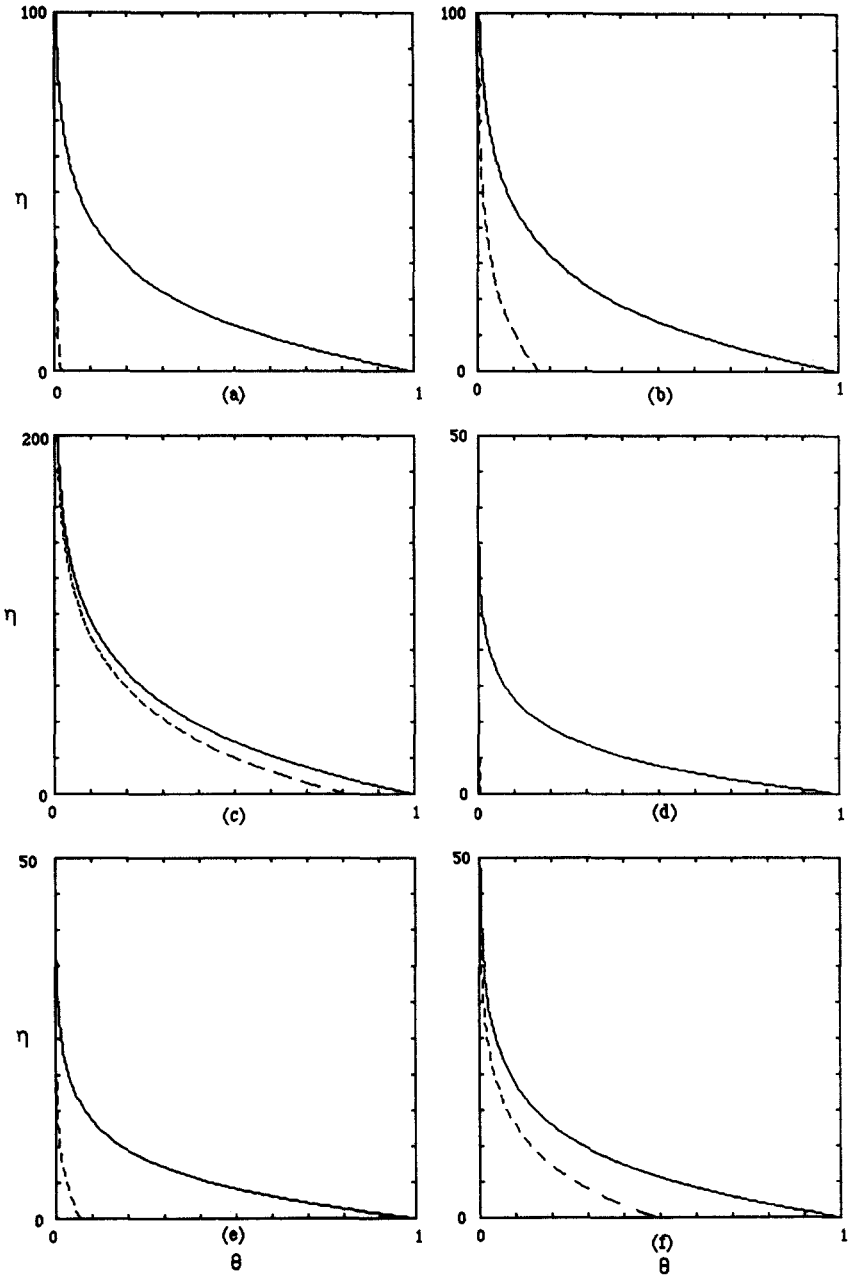

Figure 2. Stationary temperature distribution in air–particle flow. $\gamma = 10{,}000$, $\mathrm{Pr} = 0.7$. (a) $\alpha = 0.001$, $\mathrm{Re} = 1$; (b) $\alpha = 0.001$, $\mathrm{Re} = 0.1$; (c) $\alpha = 0.001$, $\mathrm{Re} = 0.01$; (d) $\alpha = 0.01$, $\mathrm{Re} = 1$; (e) $\alpha = 0.01$, $\mathrm{Re} = 0.1$; (f) $\alpha = 0.01$, $\mathrm{Re} = 0.01$. — Air, – – particles.

Temperature distributions for a mixture of water with metal particles are shown in figure 3. The depth of penetration of the temperature profiles in this case varies from 100 to 50,000 particle radii, depending on the values of α and Re, and may be up to 50 times the thickness of the boundary layer in the previous example at the same values of α and Re. The relative velocity between the phases is lower than in the case of an air–particle mixture due to a lower value of the density ratio, giving small temperature lags, detectable only in thin layers and at high values of Re, figure 3(d).

For oil–particle mixtures, illustrated in figure 4, the density ratio between the phases is the same as in the case of water. The value of $\mathrm{Pr} = 1000$ is approx. 140 times that of water. This gives thinner boundary layers and larger temperature differences than in the previous case.

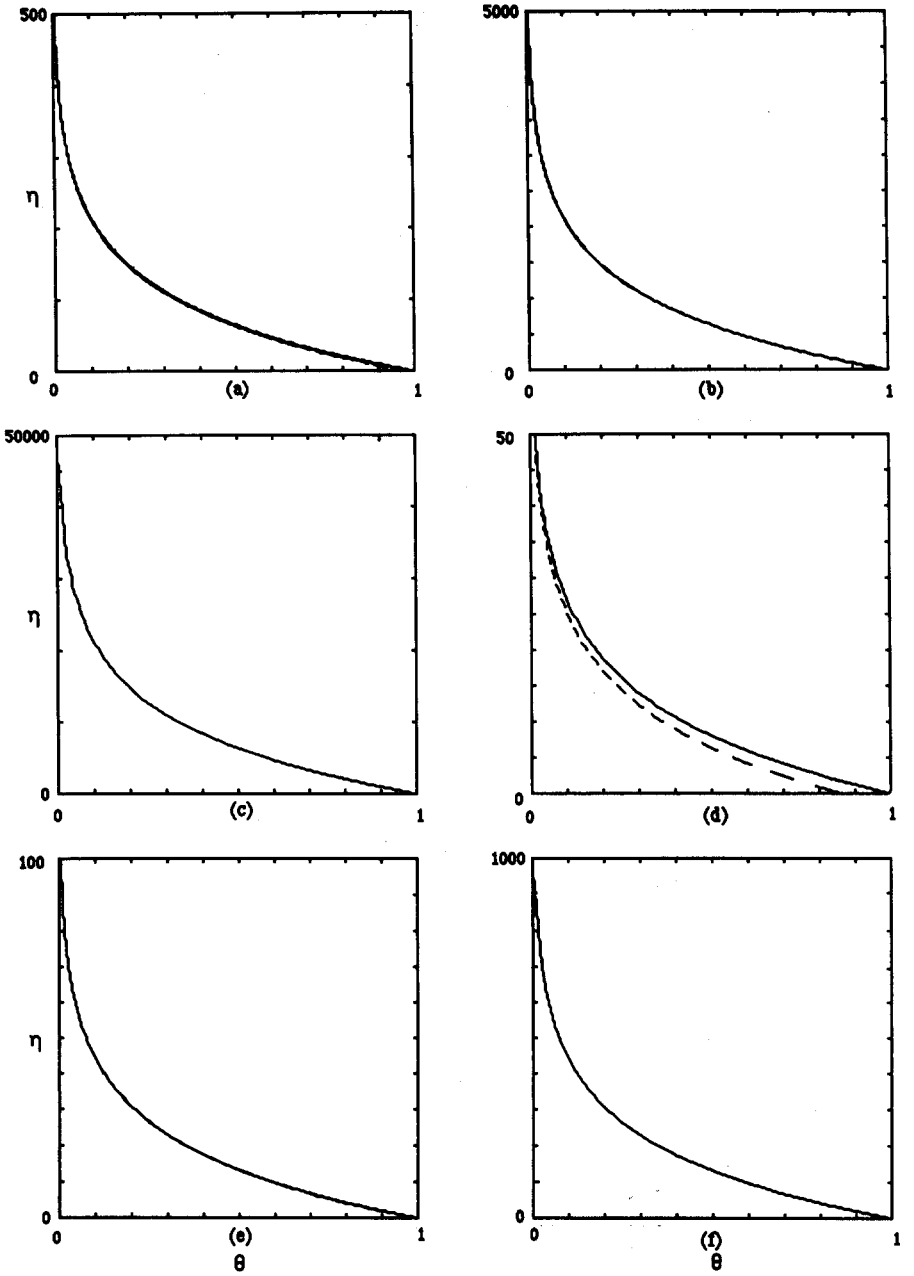

Figure 3. Stationary temperature distribution in water–particle flow. $\gamma = 10$, Pr = 7. (a) $\alpha = 0.001$, Re = 1; (b) $\alpha = 0.001$, Re = 0.1; (c) $\alpha = 0.001$, Re = 0.01; (d) $\alpha = 0.01$, Re = 1; (e) $\alpha = 0.1$, Re = 0.1; (f) $\alpha = 0.1$, Re = 0.01. — Water, -- particles.

4. PERIODIC TEMPERATURE FIELDS

Our next example is mixture flow over a periodically heated plate:

$$T_w = T_\infty + (T_w - T_\infty)\cos \omega t; \qquad [42]$$

or, in nondimensional form, the temperature of the plate varies according to

$$\theta(t, 0) = \cos \omega t. \qquad [43]$$

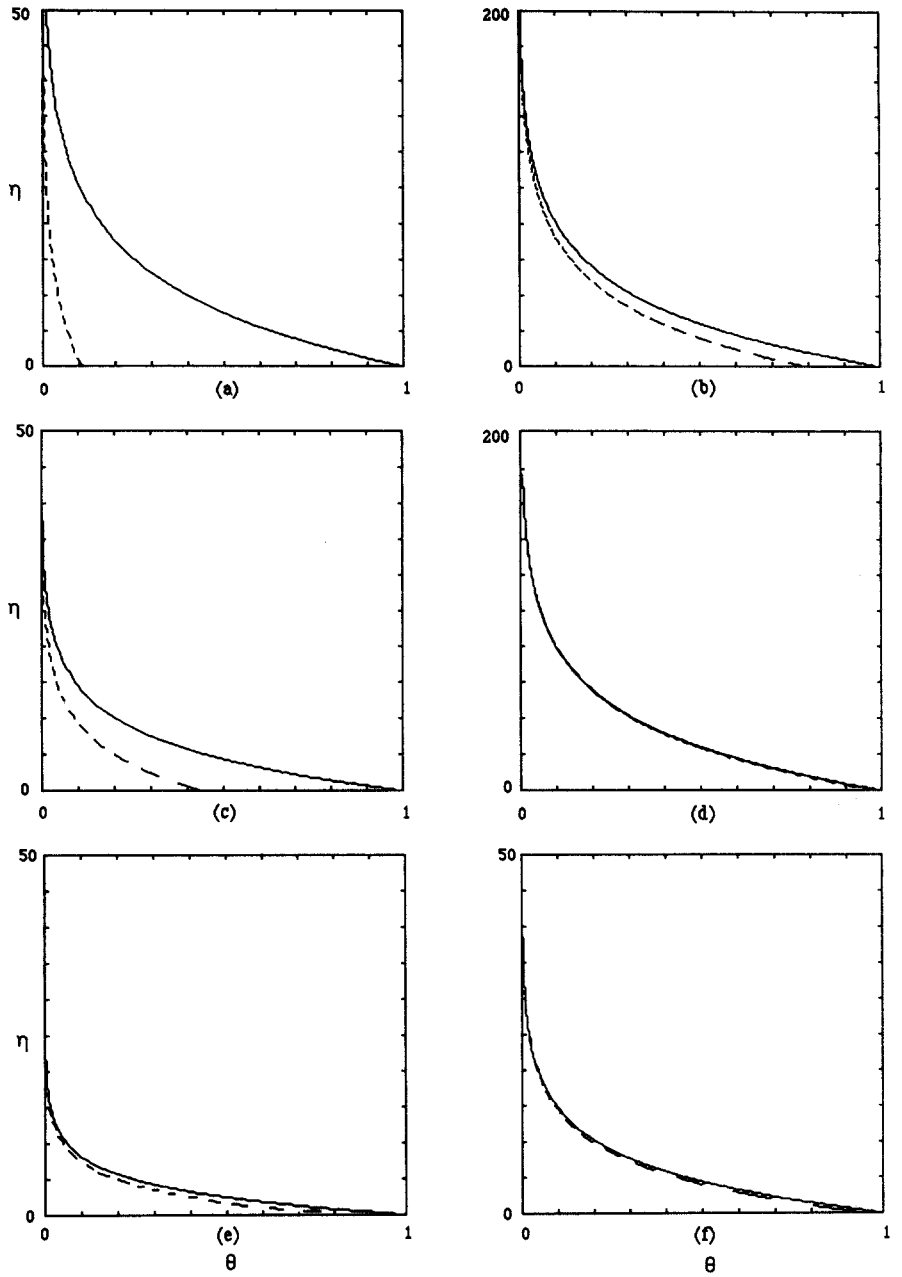

Figure 4. Stationary temperature distribution in oil–particle flow. $\gamma = 10\,\mathrm{Pr} = 1000$. (a) $\alpha = 0.001$, $\mathrm{Re} = 0.1$; (b) $\alpha = 0.001$, $\mathrm{Re} = 0.01$; (c) $\alpha = 0.001$, $\mathrm{Re} = 0.001$; (d) $\alpha = 0.01$, $\mathrm{Re} = 0.001$; (e) $\alpha = 0.1$, $\mathrm{Re} = 0.002$; (f) $\alpha = 0.1$, $\mathrm{Re} = 0.001$. — Oil, – – particles.

Thus, we will consider here a system of two energy equations,

$$A_d[\theta_{dt} - (V - V_d)\theta_{d\eta}] = \theta_c - \theta_d \qquad [44]$$

and

$$A_c[\theta_{ct} - (V - V_c)\theta_{c\eta}] = \tfrac{1}{3}\theta_{c\eta\eta} - \frac{\alpha}{1-\alpha}(\theta_c - \theta_d), \qquad [45]$$

under the boundary conditions

$$\theta_c(t, 0) = \cos \omega t \qquad [46]$$

and

$$\theta_c(t, \infty) = \theta_d(t, \infty) = 0. \qquad [47]$$

It is noteworthy that here as well as in the previous case the structure of the equations and the boundary conditions is similar to the corresponding problem of the horizontal velocity distribution in the phases, compare with Apazidis (1985). We thus seek the solution of [44]–[47] in the same form as the solution to the corresponding velocity problem, i.e.

$$\theta_c = \cos(\omega t + \mu\eta)\, e^{r\eta} \qquad [48]$$

and

$$\theta_d = [a\cos(\omega t + \mu\eta) + b\sin(\omega t + \mu\eta)]\, e^{r\eta}. \qquad [49]$$

Introducing [48] and [49] into [44] and [45] we evaluate the constants a, b, μ and r similarly to Apazidis (1985). The temperature distribution in the phases is then plotted for various values of the dimensionless parameters α, γ, Re and Pr and frequencies ω, see figures 5–13. As in the stationary case, large temperature differences between the phases are obtained at high values of the relative velocity and large relaxation times for energy transfer. Thus, large temperature differences may be expected in gas–particle mixtures with low particle concentrations and at high values of Re, due to high values of the relative velocity between the components (see figures 5 and 6), and in oil–particle mixtures, due to high values Pr (figures 11–13). For water–particle mixtures when both the relative velocity between the phase and the relaxation time for energy transfer are small, the temperature lags become insignificant. The depth of penetration of the temperature profiles, on the contrary, becomes larger (figures 8–10).

5. HEAT FLUXES

Using the obtained velocity distributions, it is now possible to evaluate the rate of heat transfer between the sediment, which has a common temperature with the plate, and the suspension. The total heat flux through the interface between the dense sediment and the mixture above it is a sum of the convective heat flux of the continuous phase and the sensible heat transfer of the particles:

$$q = q_c + q_d, \qquad [50]$$

where

$$q_c = -(1-\alpha)\kappa_c T_{cy} = -(1-\alpha)\frac{\kappa_c(T_w - T_\infty)}{a}\theta_\eta\Big|_{\eta=0} = -(1-\alpha)\frac{\kappa_c(T_w - T_\infty)}{a}r \qquad [51]$$

and

$$q_d = \alpha c_d \rho_d (v_d - v)(T_d - T_w) = \alpha c_d \rho_d \frac{ga^2\gamma}{\nu_c}(T_w - T_\infty)(V_d - V)(\theta_d - 1), \qquad [52]$$

which gives

$$q = c_c\rho_c\frac{\kappa_c}{a}(T_w - T_\infty)[-(1-\alpha)r + \alpha k\gamma\,\mathrm{RePr}(V_d - V)(\theta_d - 1)] \qquad [53]$$

or

$$q = c_c\rho_c\frac{\kappa_c}{a}(T_w - T_\infty)[Q_c - Q_d], \qquad [54]$$

with

$$Q_c = -(1-\alpha)r \quad \text{and} \quad Q_d = \alpha k\gamma\,\mathrm{RePr}(V_d - V)(\theta_d - 1) \qquad [55]$$

being the dimensionless heat fluxes due to convection and sensible heat transfer, respectively. Here, $-r$ ($r < 0$) is the Nusselt number for the continuous phase.

Plots of the dimensionless heat fluxes of the continuous and dispersed phases as well as the total ones are displayed in figures 14 and 15. Figures 14(a,b) show heat fluxes, in the case of a gas–particle mixture, as a function of α and at various values of Re. For low values of Re, as in figure 14(a), the total heat flux is almost entirely due to the convective heat transfer of the continuous phase. When the value of Re becomes >0.1, as in figures 14(c,d), the situation is reversed and the total

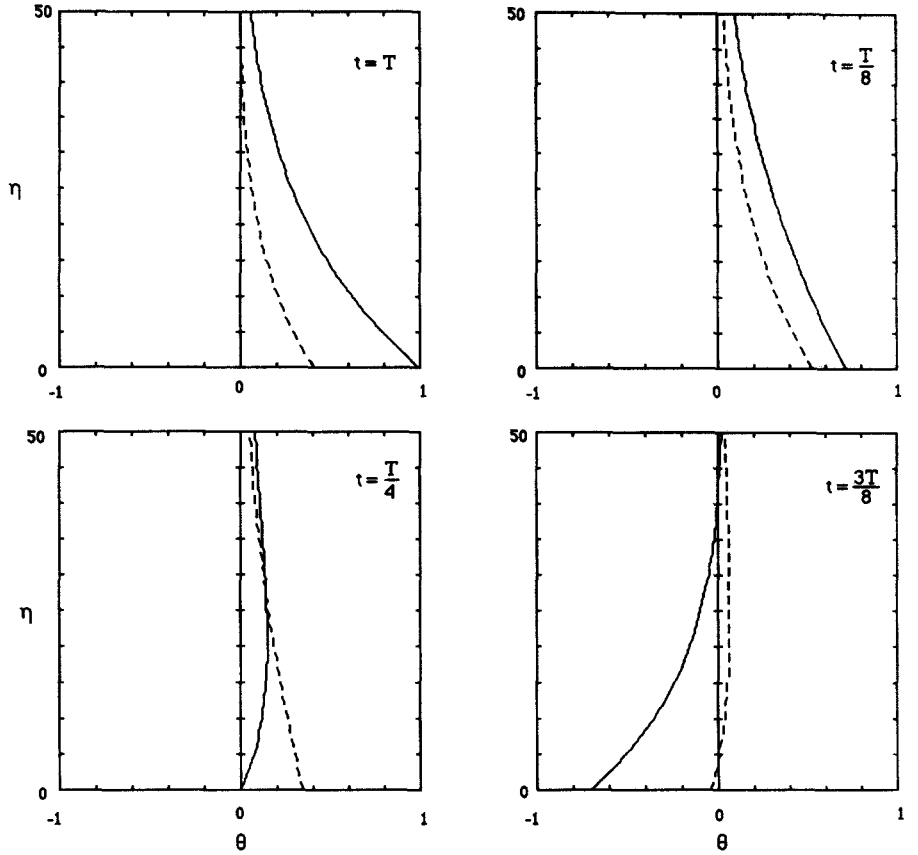

Figure 5. Periodic temperature distribution in air–particle flow. $\gamma = 10{,}000$, Pr = 0.7, $\alpha = 0.001$, Re = 0.01, $\omega = 0.1$. — Air, – – particles.

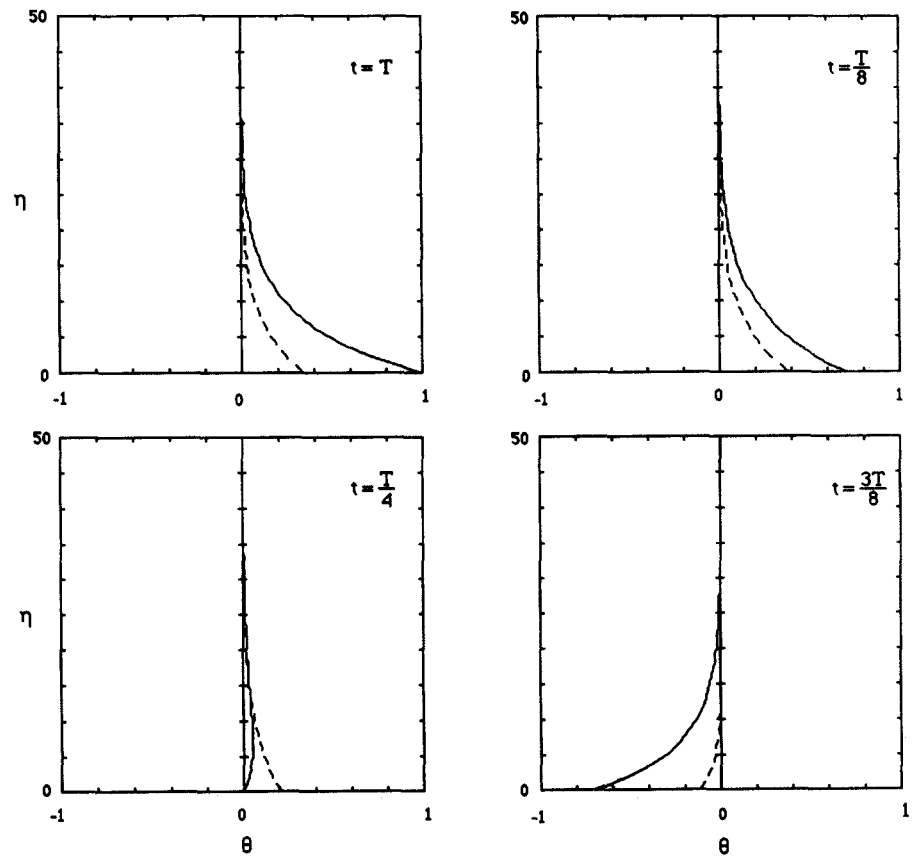

Figure 6. Periodic temperature distribution in air–particle flow. $\gamma = 10{,}000$, Pr = 0.7, $\alpha = 0.01$, Re = 0.01. $\omega = 0.1$. — Air, – – particles.

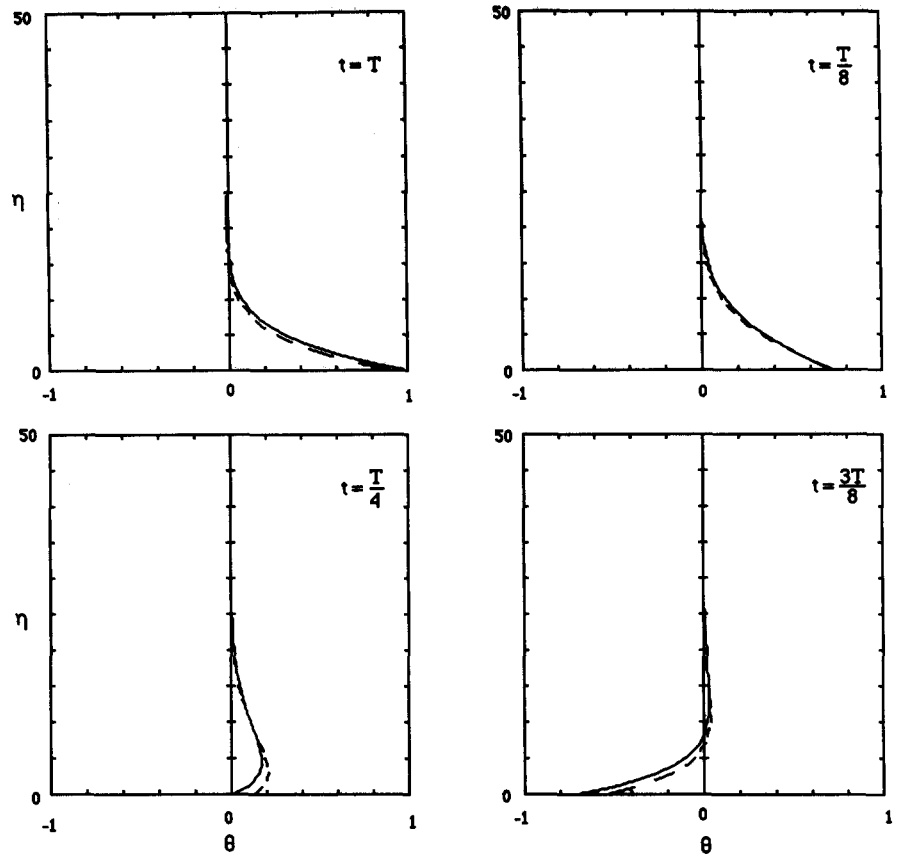

Figure 7. Periodic temperature distribution in air–particle flow. $\gamma = 10{,}000$, $\mathrm{Pr} = 0.7$, $\alpha = 0.1$, $\mathrm{Re} = 0.001$, $\omega = 0.1$. — Air, -- particles.

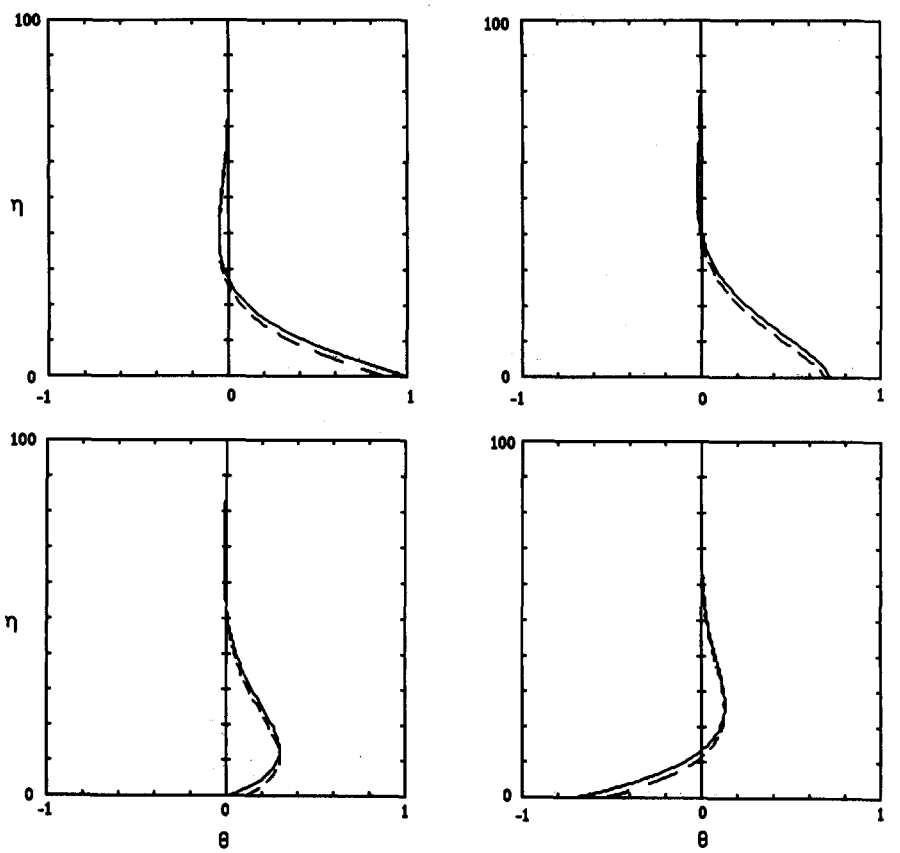

Figure 8. Periodic temperature distribution in water–particle flow. $\gamma = 10$, $\mathrm{Pr} = 7$, $\alpha = 0.001$, $\mathrm{Re} = 1$, $\omega = 0.001$. — Water, -- particles.

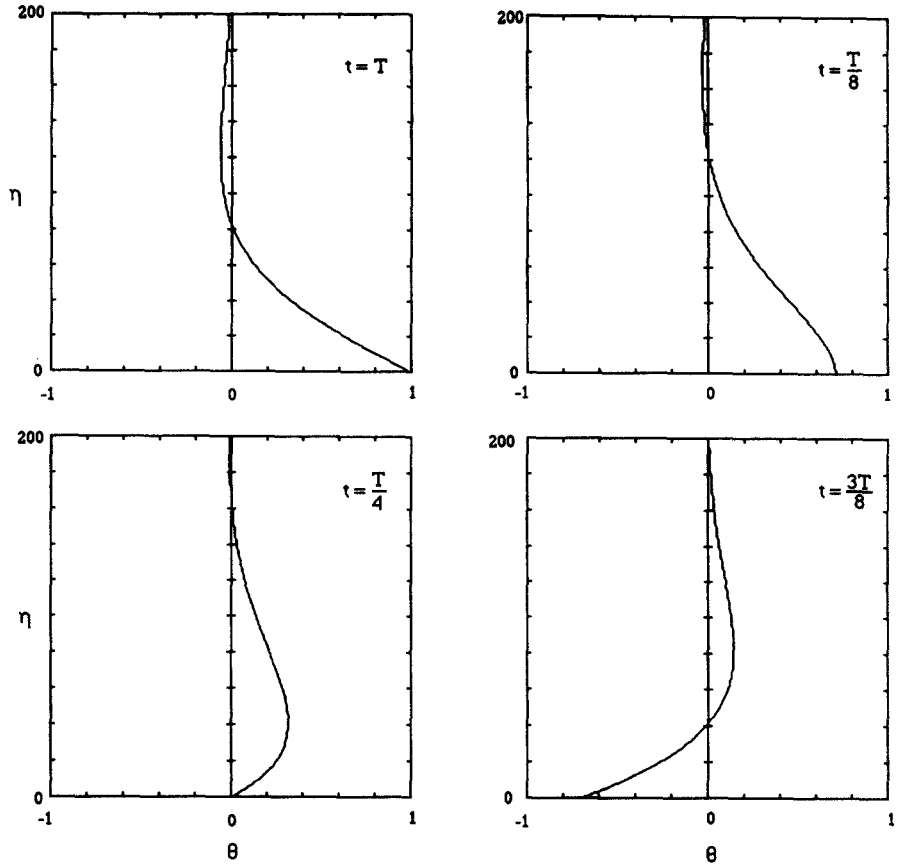

Figure 9. Periodic temperature distribution in water–particle flow. $\gamma = 10$, $\mathrm{Pr} = 7$, $\alpha = 0.001$, $\mathrm{Re} = 0.1$, $\omega = 0.001$. — Water, – – particles.

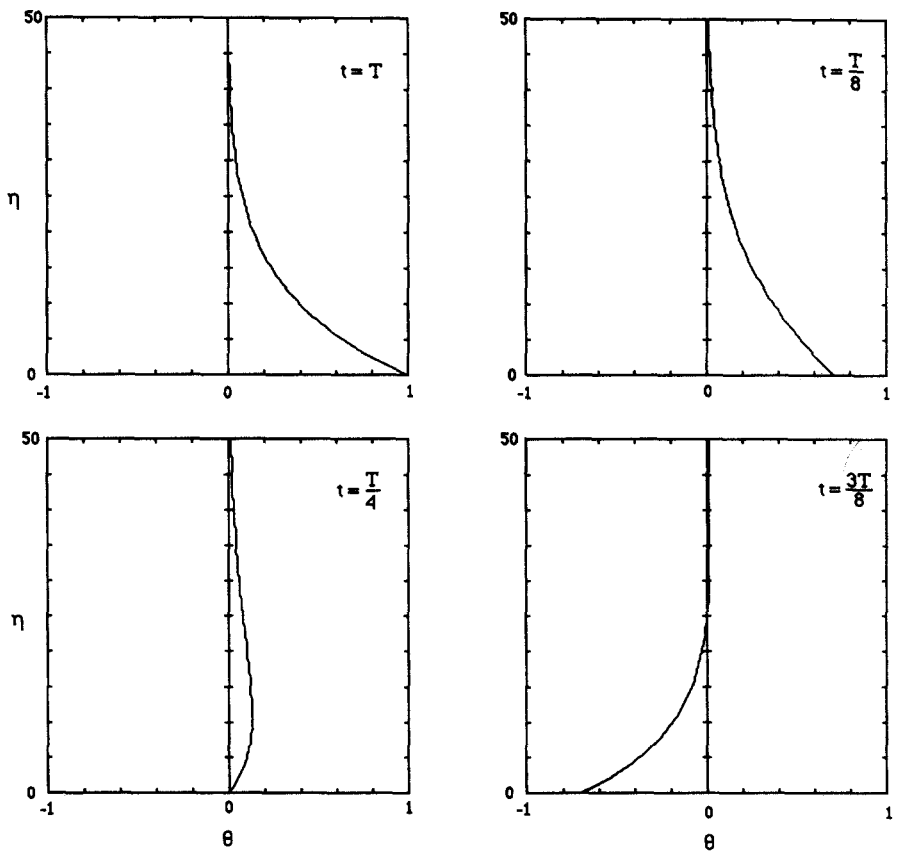

Figure 10. Periodic temperature distribution in water–particle flow. $\gamma = 10$, $\mathrm{Pr} = 7$, $\alpha = 0.1$, $\mathrm{Re} = 0.1$ $\omega = 0.01$. — Water, – – particles.

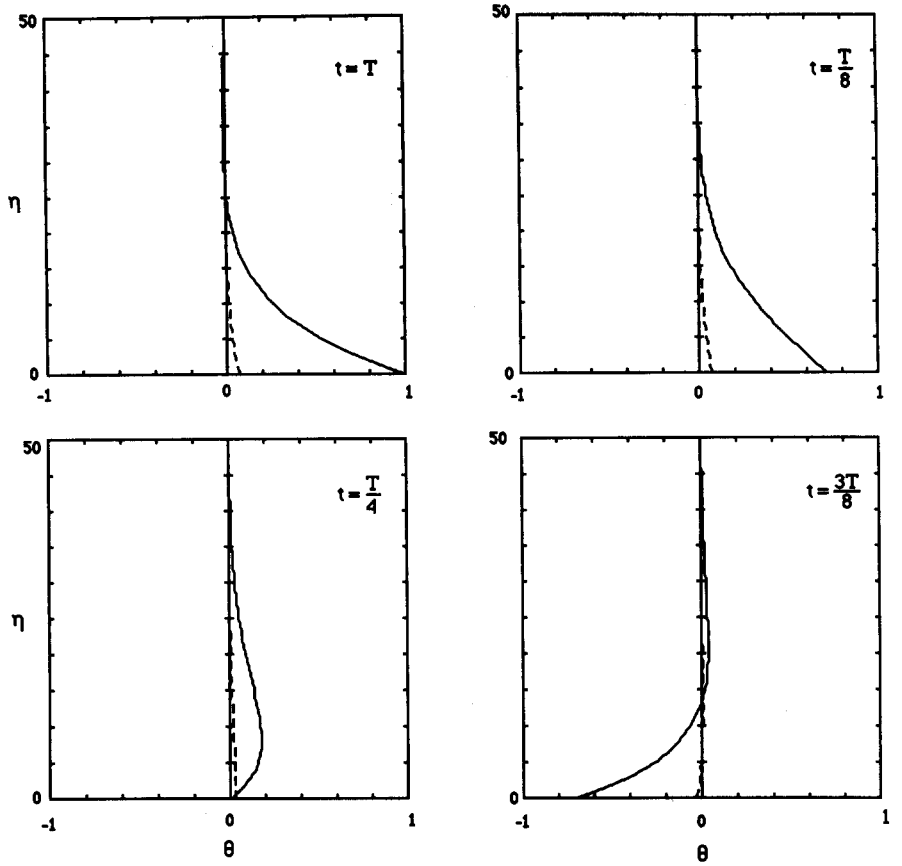

Figure 11. Periodic temperature distribution in oil–particle flow. $\gamma = 10$, Pr = 1000, $\alpha = 0.001$, Re = 0.1, $\omega = 0.0001$. — Oil, -- particles.

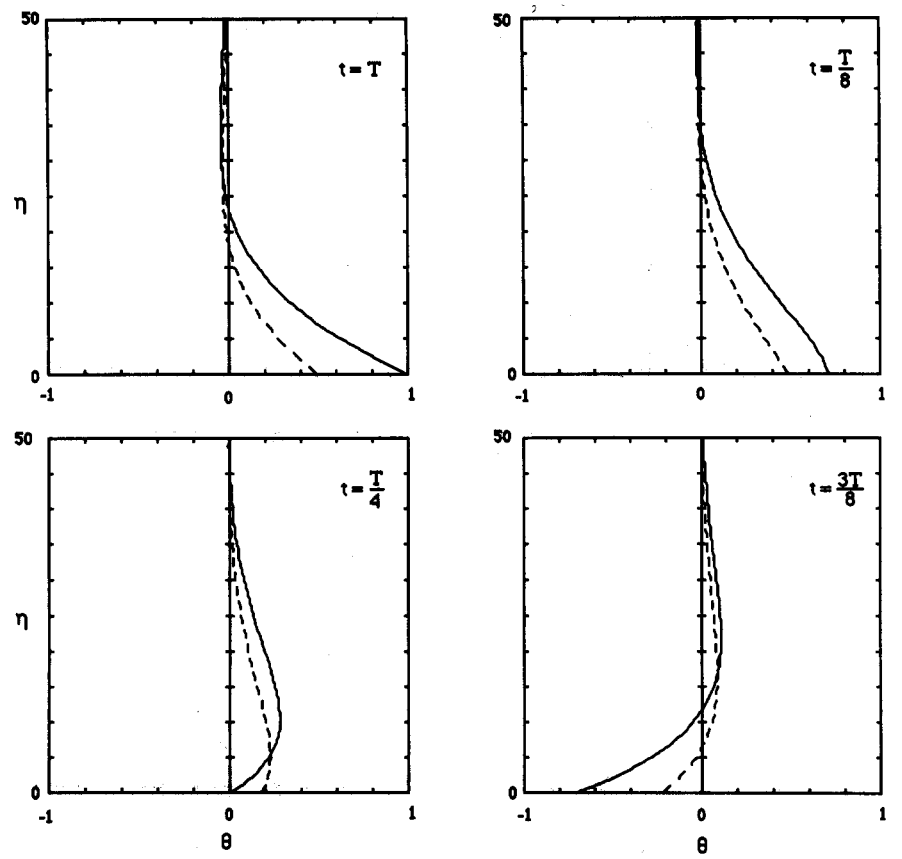

Figure 12. Periodic temperature distribution in oil–particle flow. $\gamma = 10$, Pr = 1000, $\alpha = 0.001$, Re = 0.01, $\omega = 0.001$. — Oil, -- particles.

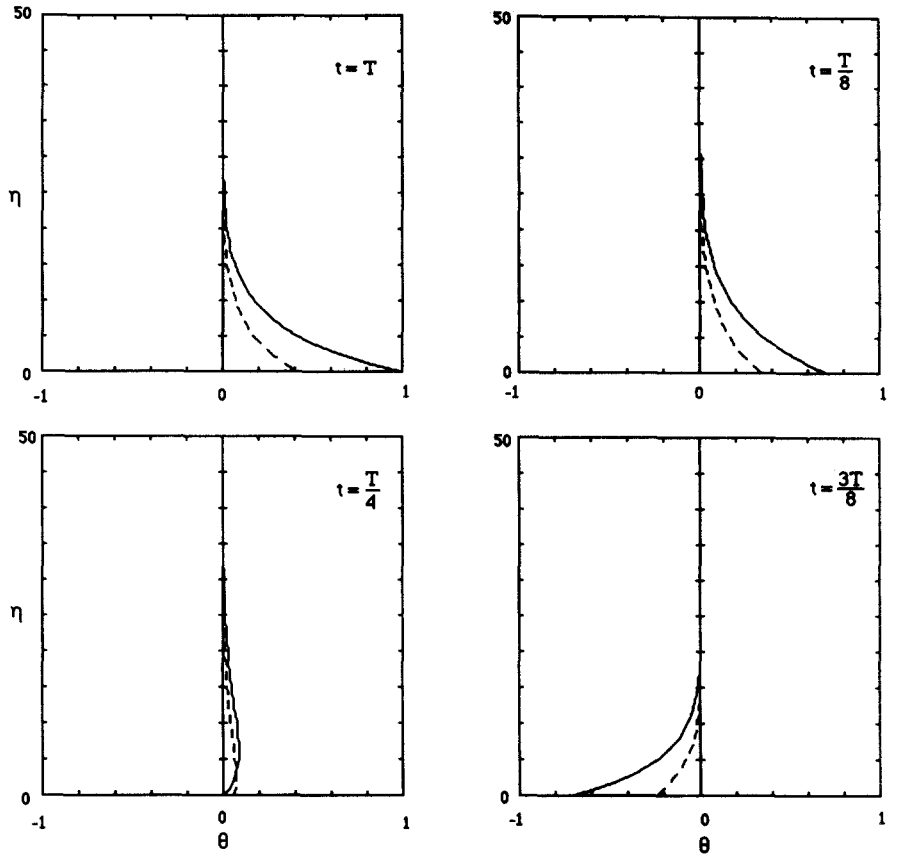

Figure 13. Periodic temperature distribution in oil–particle flow. $\gamma = 10$, Pr = 1000, $\alpha = 0.01$, Re = 0.01, $\omega = 0.001$. — Oil, – – particles.

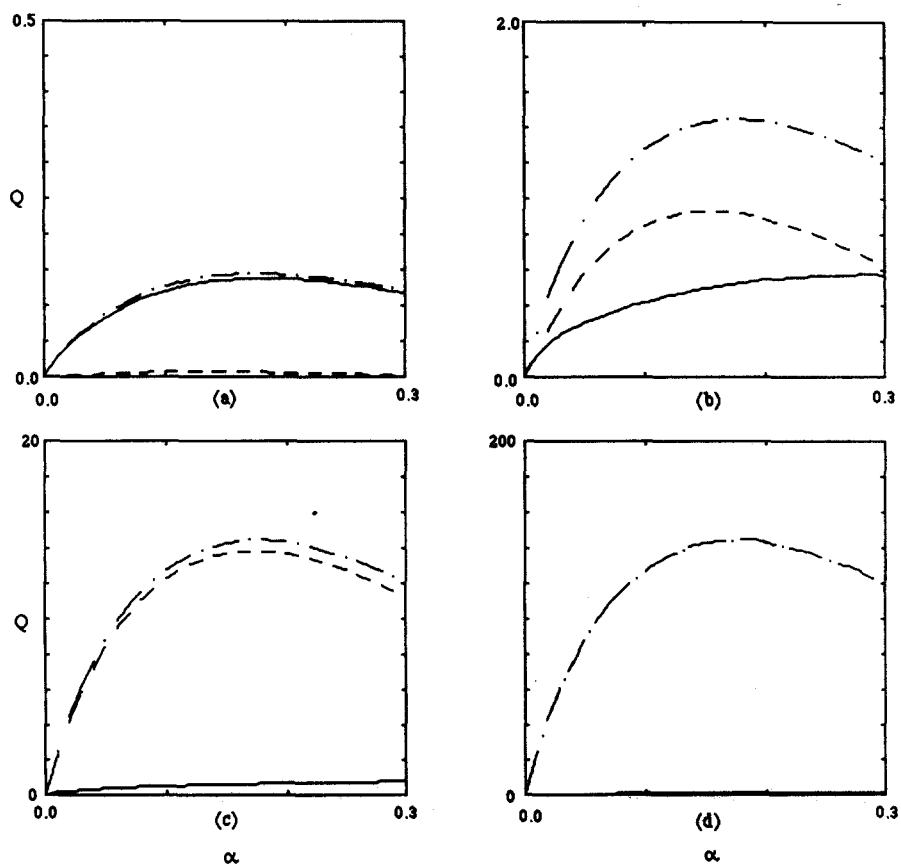

Figure 14. Heat fluxes vs volume fraction of particles in air–particle flow. $\gamma = 10{,}000$, Pr = 0.7. (a) Re = 0.001, (b) Re = 0.01, (c) Re = 0.1, (d) Re = 1. — Air, – – particles, – · – total.

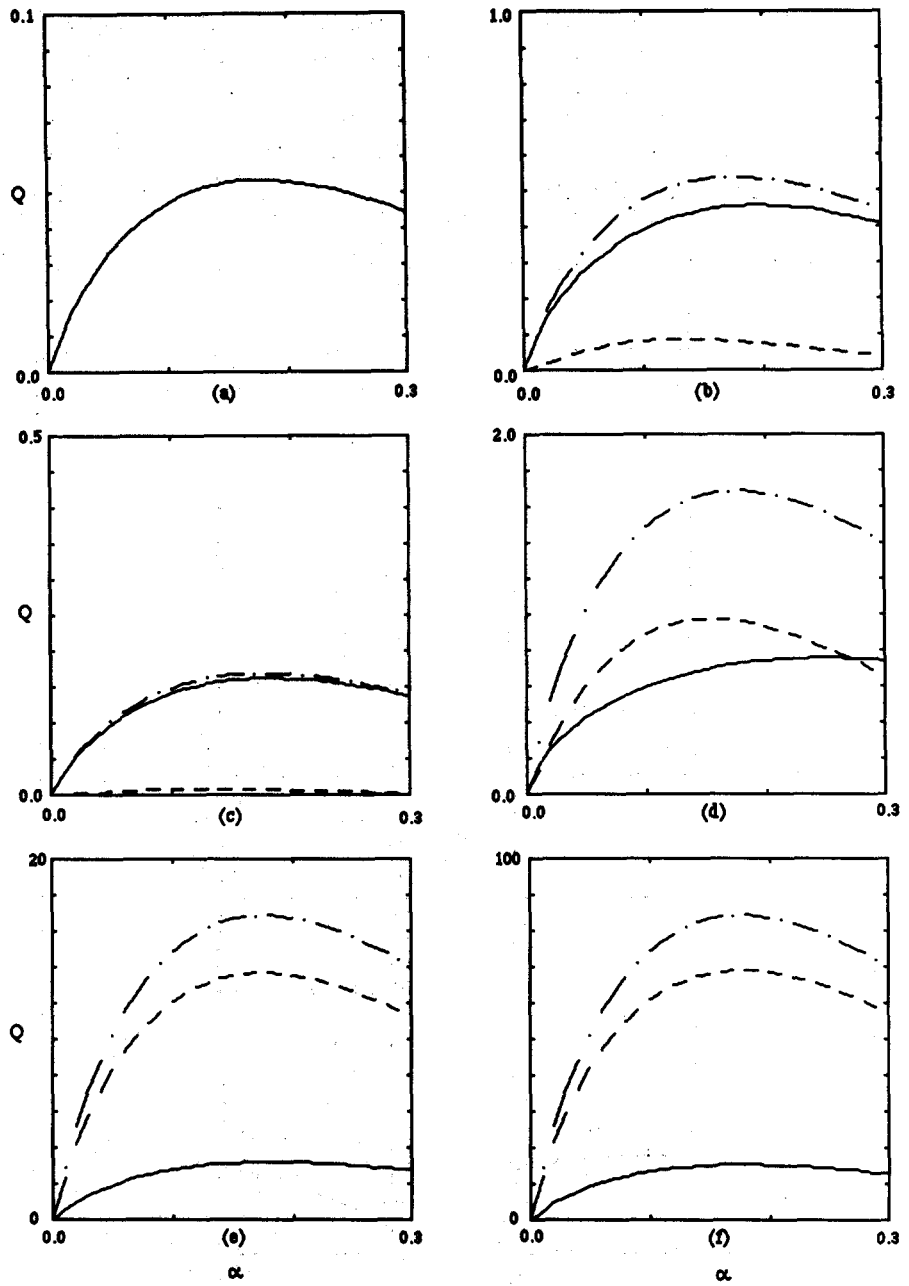

Figure 15. Heat fluxes vs volume fraction of particles. (a) Water–particle mixture, $\gamma = 10$, Pr = 7, Re = 0.1; (b) $\gamma = 10$, Pr = 7, Re = 1. (c) Oil–particle mixture, $\gamma = 10$, Pr = 1000, Re = 0.001. (d) Oil–particle mixture, $\gamma = 10$, Pr = 1000, Re = 0.01. (e) Oil–particle mixture, $\gamma = 10$, Pr = 1000, Re = 0.01. (f) Oil–particle mixture, $\gamma = 10$, Pr = 1000, Re = 0.5. — Liquid, – – – particles, – · – total.

heat flux stems mainly from the sensible heat transfer due to particle impingement on the sediment layer. At greater values of Re, the relative velocity increases and the particles need less time to travel through the region of the thermal boundary layer, thus preserving the lower temperature of the regions away from the interface, see figures 2(a,b). This results in a greater temperature difference between the impinging particles and the sediment and thus a higher rate of heat transfer.

Figure 13 shows heat fluxes for water–particle and oil–particle mixtures as a function of α. Here the density ratio between the fluid and solid phases is the same but the value of Pr for oil is chosen to be 140 times greater than for water. Consequently, the thickness of the thermal boundary layer for the oil–particle mixture, at the same values of α and Re, approx. 100 times less than for the water–particle suspension, cf. figures 3(b) and 4(a). The heat flux in water–particle mixtures is thus

mainly due to the convective heat transfer in the continuous phase, whereas in the case of oil–particle mixtures this is true only at low values of the particle Re, as in figure 15(c). At higher values of Re the heat flux becomes dominated by the sensible heat transfer of the particles, see figure 15(f).

Figures 14 and 15 also suggest that the rate of heat transfer in the suspension does not simply increase with an increase in α, but reaches a maximum at a value of $\alpha = 0.2$ and decreases with a further increase in α. This has a straightforward explanation in cases when the heat flux is mainly due to the sensible heat transfer of particles. According to [55] the sensible heat transfer of impinging particles is proportional to the volume fraction of the particles, the relative velocity between the particles and the interface and the temperature difference between the particles and the interface. An increase in α initially gives an increase in the heat flux rate. An increase in α leads, however, to an increase in the interaction force between the phases, which results in lower values of the relative velocity and an increase in the times needed for particles to travel through the boundary layer region, and thus smaller temperature differences between the impinging particles and the interface. At a certain value of α the effect of a decrease in the values of the relative velocity and temperature difference becomes greater than the effect of an increase in α on the heat flux and the heat flux diminishes.

A maximum of the heat transfer rate exists, however, also in the cases when the heat flux is mainly due to a convective heat transfer in the continuous phase, as in figures 14(a) and 15(a,c). Dimensionless convective heat flux is, according to [55], equal to the volume fraction of the continuous phase times the Nusselt number, or the dimensionless temperature gradient of the continuous phase at the interface. An increase in α leads initially to an increase in the heat transfer between the phases, which results in higher temperature gradients in the continuous phase at the interface. A further increase in α gives, however, lower values of the relative velocity between the phases and thus lower temperature differences, leading to lower temperature gradients in the continuous phase at the interface.

6. CONCLUSIONS

An analysis of the temperature distribution and heat transfer in a laminar two-phase mixture flow over a heated horizontal plate has been carried out. We summarize here the main items of the present investigation.

(1) The temperature profiles of both phases span over a region existing at the interface between the dense sediment collected on the plate and the mixture above it. This region, together with the interface, propagates in the upward direction with a constant velocity, defined by the particle size and concentration as well as the density ratio between the phases.

(2) The vertical motion of the phases and of the interface is independent of the horizontal motion and allows a temperature distribution with a structure more simple than its single-phase counterpart and similar to the velocity distribution over a flat plate at zero incidence with uniform suction. Unlike the single-phase case, the temperature profiles in the two-phase mixture are independent of the distance along the plate. Another simplification, as compared with the single-phase case, is that the temperature distribution in the two-phase boundary layer is independent of the horizontal velocity components of the phases.

(3) Large temperature differences between the phases are to be found in thin (20–100 particle radii) boundary layers which exist at high density ratios between the phases (heavy particles in gas), large values of Re (large particle sizes) or high values of Pr (oil–particle mixtures).

(4) Thick boundary layers (100 particle radii and more) exist at low particle concentrations (of order of 0.01), lower values of the density ratio (e.g. particles in liquids), low values of Pr (water–particle mixtures) and low values of Re (small particle sizes).

(5) The total heat flux in the two-phase mixture is not simply increased by an increase in α, but reaches a maximum at $\alpha = 0.2$ and decreases with a further increase in α.

REFERENCES

APAZIDIS, N. 1985 On two-dimensional laminar flows of a particulate suspension in the presence of gravity field. *Int. J. Multiphase Flow* **11,** 657–698.

APAZIDIS, N. 1988 Gas–particle flow in a deep vertical cavity due to thermal convection and phase separation. *Int. J. Multiphase Flow* **14,** 607–631.

BENNON, W. D. & INCROPERA, F. P. 1987 A continuum model for momentum, heat and species transport in binary solid–liquid phase change systems—I. Model formulation. *Int. J. Mass Heat Transfer* **40,** 2161–2170.

DREW, D. A. 1979 Application of general constitutive principles to the derivation of multi-dimensional two-phase flow equations. *Int. J. Multiphase Flow* **5,** 243–246.

DREW, D. A. 1983 Mathematical modelling of two-phase flow. *A. Rev. Fluid Mech.* **15,** 261–291.

DRUMHELLER, D. S. & BEDFORD, A. 1980 On the mechanics and thermodynamics of fluid mixtures. *Archs ration. Mech. Analysis* **73,** 257–284.

ISHII, M. 1975 *Thermo-fluid Dynamic Theory of Two-phase Flow.* Eyrolles, Paris.

ISHII, M., UMEDA, Y. & KAWASAKI, K. 1987 Nozzle flows of gas–particle mixtures. *Phys. Fluids* **30,** 752–760.

RUBINOW, S. I. & KELLER, J. B. 1961 The transverse force on a spinning sphere moving in a viscous fluid. *J. Fluid Mech.* **11,** 447–459.

SAFFMAN, P. G. 1965 The lift on a small sphere in a slow shear flow. *J. Fluid Mech.* **22,** 385–400.

SCHLICHING, H. 1968 *Boundary-layer Theory.* McGraw-Hill, New York.

SHA, W. T. & SOO, S. L. 1978 Multidomain multiphase fluid mechanics. *Int. J. Heat Mass Transfer* **21,** 1581–1595.

SOO, S. L. 1965 *Fluid Dynamics of Multiphase Systems.* Blaisdell, Waltham, Mass.

TAM, K. W. 1969 The drag on a cloud of spherical particles in low Reynolds number flow. *J. Fluid Mech.* **38,** 537–546.

WALLIS, G. B. 1969 *One-dimensional Two-phase Flow.* McGraw-Hill, New York.

ZUBER, N. 1964 On the dispersed two-phase flow in a laminar flow region. *Chem. Engng Sci.* **19,** 897–917.